

# STATIC AND DYNAMIC RESPONSE OF CARBON NANOTUBE-BASED NANO-TWEEZERS

R. Shabani\*, N. sharafkhani and V. M. Gharebagh

Department of Mechanical Engineering, Urmia University, Urmia, Iran. P.O. Box: 165, Urmia, Iran  
r.shabani@urmia.ac.ir, n.sharafkhani@gmail.com, V.gharebagh@gmail.com

\*Corresponding Author

(Received: July 30, 2011 – Accepted in Revised Form: October 20, 2011)

doi: 10.5829/idosi.ije.2011.24.04a.06

**Abstract** In this paper static and dynamic responses of a nano-tweezer composed of two carbon nano-tube (CNT) arms are investigated. Taking into account a continuum model and considering the electrostatic actuation as well as the presence of the van der Waals forces, the static nonlinear equations are solved by a step by step linearization and Galerkin projection method. Simulating the closing dynamics of the nano-tweezer, the specified effective diameters of the nanotubes compared to existing experimental data. Then by imposing a step DC voltage and taking into account the inertia effects, the dynamic responses and pull-in conditions of the nano-tweezer are studied. In the static and dynamic analysis, the effects of various parameters such as initial gap, length and diameter of the nanotubes on the pull-in conditions are investigated. Also the effect of damping and asymmetric stiffness of the arms on the pull-in voltages of the nano-tweezer is reported. Comparison of the results with the published experimental data shows that the use of continuum model and employing the Galerkin based step by step linearization method (SSLM) could effectively simulate the response of nano-tweezers.

**Keywords** Nano-tweezer, Dynamic analysis, Pull-in voltage, Nanotube

**چکیده** در این مقاله پاسخ استاتیکی و دینامیکی یک نانو انبرک که متشکل از دو نانو لوله کربنی یک سر درگیر می باشد مورد بررسی قرار گرفته است. با در نظر گرفتن نیروی بین مولکولی و اندروالس و تحریک الکترواستاتیکی، مدل پیوسته برای نانولوله ها استخراج شده و از طریق روش خطی سازی گام به گام و به کار گیری روش گلرکین حل شده اند. با شبیه سازی عملکرد نانو انبرک، قطر موثر نانولوله های مربوطه محاسبه شده و با نتایج آزمایشگاهی مورد مقایسه قرار گرفته است. در ادامه با اعمال ولتاژ تحریک به فرم پله و لحاظ کردن نیروهای اینرسی پاسخ دینامیکی و ناپایداری نانو انبرک مربوطه مشخص گردیده است. در تحلیل فوق اثرات پارامترهای مختلف نظیر فاصله اولیه بین نانولوله ها، طول و قطر نانولوله ها و شرایط عدم تقارن آنها بر روی عملکرد و پایداری سیستم مورد بررسی قرار گرفته است. مقایسه نتایج به دست آمده با نتایج آزمایشگاهی نشان داده است که استفاده از روش خطی سازی گام به گام به همراه روش گلرکین روشی موثر جهت تحلیل نانو انبرکها می باشد.

## 1. INTRODUCTION

Since the discovery of carbon nanotubes [1] they have been widely used in many nano electromechanical systems (NEMS). Nanotubes properties depend on atomic arrangement, their diameter and length. They have high aspect ratio, flexibility and thermal and chemical stability. Nanotubes exist as single-walled or multi-walled structures, where the multi-walled nanotubes (MWNT) are composed of multiple concentric single-walled carbon nanotubes (SWCN). Because of their aforementioned properties they have been

used in many nanoscale applications. They have been utilized as resonators [2], nanorelays [3,4], and electrostatic switches [5, 6]. Moreover the nanotubes have been used as rotational elements in nano rotational motors [7], and in a special type of random access memory they used as suspended elements which operates as switches [8]. The SWCN in the form of fixed-fixed and fixed-free is also used as mass sensor [9]. Moreover they were used in atomic force microscopy to measure the force between solid surfaces, where in some cases it could be interacts with the surrounding liquid, where in addition to intermolecular forces, the

osmotic forces should also be considered [10].

Nano-tweezers are also nanotube-based devices composed of two cantilever carbon nanotube arms. They are used for manipulation of nanostructures and two-tip scanning-tunneling microscope (STM) or atomic force microscope (AFM) [11, 12].

Electrostatic actuation is commonly used to actuate nano-tweezers, where in the gaps smaller than 30 nm the van der Waals forces become detrimental. Based on this type of actuation some experiments have been done on the nanotube-based devices. In an experiment S. Akita *et al.* developed a nano-tweezer consisting of carbon nanotube arms and operated it in an AFM [12]. By imposing various DC voltages between the arms they derived the deflections of the arms as function of the applied voltage and verified their results employing a continuum model and extracted an effective diameter for arms. Lee and Kim proposed a new type of nano-tweezer [13], where each arm had a separated substrate. Based on a continuum model and ignoring the dynamic terms, they compared the simulation and experimental load deflection curves. In another experiment H. D. Espinosa *et al.* employed energy method for predictions of pull-in voltage in a nanotube-based nanoswitch. Considering small and finite deflection models they have shown the effectiveness of the energy method in predictions of structural behavior and pull-in voltages of nanosystems [14, 15]. Due to complexity of experiment on NEMS structure, many simulations have been done in the predictions of the structural behavior of the NEMS devices. In a static analysis and taking into account the van der Waals force, Wang *et al.* have studied the stability of a nanotube-based nano-tweezer [16]. Using continuum model and employing the Galerkin method, they have studied the pull-in conditions and the detachment length of the arms. In an extensive study Dequesnes and coworkers investigated nanotube-based switches using molecular dynamics (MD) and continuum model [17]. By numerical simulations based on domain discretization, they have shown that the results of a linear continuum model closely match the experimental data reported for nano-tweezers. Taking into account the dynamic effects and considering the MD model near the clamped supports and continuum model far from the supports, they extracted the load deflection curves

[18]. They have concluded that the combined MD/nonlinear continuum approach is adequate for double clamped nanotubes and the linear continuum model is acceptable for cantilever types. Taking into account dispersion forces, Ramezani [19] investigated the pull-in instability of the nano-tweezers using distributed and lumped parameter models. By analogy to nano-switches, they proposed a closed-form solution and determined the detachment length and minimum initial gap of the nano-tweezers.

In this paper a nano-tweezer with two SWCN arms is considered. The proposed model takes into account the nonlinear electrostatic and van der Waals forces. The nonlinear governing equations are extracted and linearized using SSLM method. In each step of linearization the Galerkin based reduced-order method is used for solving the equations. Then taking into account the acceleration terms and employing the proposed numerical method (Galerkin based SSLM method) the dynamic analysis is performed and by imposing various step DC voltages the dynamic closing of the nano-tweezer arms are simulated. Simulations are carried out for various arms parameters in symmetric and asymmetric cases.

## 2. MATHEMATICAL MODELING

Figure 1 depicts the schematic view of a SWCN nano-tweezer. The cantilever arms are approached each other when a voltage difference  $V$  is applied between them.

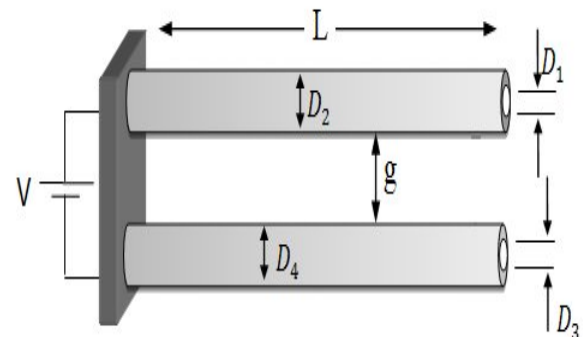


Figure 1. Schematic view of the nano-tweezer.

In small gaps ( $g$ ), less than 30 nanometers, besides the electrostatic force the van der Waals force could have considerable effects on the deflections of the arms, where in large gapes the effects of this force can be neglected [17]. In the present model  $R_1$  and  $R_3$  are internal radii and  $R_2$  and  $R_4$  are the external radii of the SWCN's. Due to uncertainty in real applications the arms of nano-tweezers could have different specification such as bending rigidity, diameter, clamped conditions, etc. [12]. So in the numerical simulations different specifications are assumed for each arm and subscripts  $a$  and  $b$  are used to denote each one. Based on continuum model the governing equations of the arms can be written as;

$$(EI)_a \frac{\partial^4 w_a}{\partial x^4} + \rho A_a \frac{\partial^2 w_a}{\partial t^2} + c_a \frac{\partial w_a}{\partial t} = F_e + F_V \quad (1)$$

$$(EI)_b \frac{\partial^4 w_b}{\partial x^4} + \rho A_b \frac{\partial^2 w_b}{\partial t^2} + c_b \frac{\partial w_b}{\partial t} = F_e + F_V$$

where  $(EI)_i$  are the bending rigidity and  $w_i$  are the lateral deflections of the arms. Also  $\rho_i$  and  $A_i$  are the mass density and cross sections of the arms. In real applications the system could be subject to a damping, where it is approximated by an equivalent damping coefficient  $c_i$  per unit length. The forcing terms  $F_e$  and  $F_V$  are the electrostatic and van der Waals forces and have the following form [16, 17]:

$$F_e = \frac{\varepsilon_0 \pi V^2}{R \sqrt{\frac{S(S+2R)}{R^2}} \left[ \ln \left( 1 + \frac{S}{R} + \sqrt{\frac{S(S+2R)}{R^2}} \right) \right]^2} \quad (2)$$

$$F_V = \frac{A_H}{8\sqrt{2}} \left[ \frac{1}{(S)^{5/2}} \left( \frac{R_2 R_4}{R_2 + R_4} \right)^{1/2} - \frac{1}{(S+T)^{5/2}} \left( \frac{R_2 R_3}{R_2 + R_3} \right)^{1/2} - \frac{1}{(S+T)^{5/2}} \left( \frac{R_1 R_4}{R_1 + R_4} \right)^{1/2} + \frac{1}{(S+2T)^{5/2}} \left( \frac{R_1 R_3}{R_1 + R_3} \right)^{1/2} \right]$$

where  $T$  is the thickness of the nanotubes. In the electrostatic force  $F_e$  the radius  $R$  could be replaced by the external radii of the arms  $R_2$  or  $R_4$ . In which  $\varepsilon_0$  and  $A_H$  are the domain permittivity and Hamaker constants respectively and  $S$  is the distance between the nanotubes,  $S = g - w_a - w_b$ . Now by introducing the following nondimensional parameters;

$$\hat{x} = \frac{x}{l}, \hat{w} = \frac{w}{g}, \hat{t} = \frac{t}{t^*}, \hat{c} = \frac{c}{t^* EI / L^4}, t^* = \sqrt{\rho A l^4 / EI} \quad (3)$$

the governing equations could be written as:

$$\frac{\partial^4 \hat{w}_a}{\partial \hat{x}^4} + \frac{\partial^2 \hat{w}_a}{\partial \hat{t}^2} + \hat{c} \frac{\partial \hat{w}_a}{\partial \hat{t}} = \alpha_1 \hat{F}_E + \alpha_2 \hat{F}_V \quad (4)$$

$$\frac{\partial^4 \hat{w}_b}{\partial \hat{x}^4} + \frac{\partial^2 \hat{w}_b}{\partial \hat{t}^2} + \hat{c} \frac{\partial \hat{w}_b}{\partial \hat{t}} = \alpha_1 \hat{F}_E + \alpha_2 \hat{F}_V$$

where  $\alpha_1, \alpha_2$  and the transformed forcing terms are defined as:

$$\alpha_1 = \frac{\varepsilon_0 \pi L^4}{(EI)(g^2)}; \alpha_2 = \frac{A_H L^4}{8\sqrt{2}(EI)(g^{3.5})}$$

$$\hat{F}_e = \frac{v^2}{R \sqrt{\frac{\hat{S}(\hat{S}+2R/g)}{R^2}} \left[ \ln \left( 1 + \frac{g\hat{S}}{R} + \sqrt{\frac{g^2 \hat{S}(\hat{S}+2R/g)}{R^2}} \right) \right]^2}$$

$$\hat{F}_V = \left[ \frac{1}{(\hat{S})^{5/2}} \left( \frac{R_2 R_4}{R_2 + R_4} \right)^{1/2} - \frac{1}{(\hat{S}+T/g)^{5/2}} \left( \frac{R_2 R_3}{R_2 + R_3} \right)^{1/2} - \frac{1}{(\hat{S}+T/g)^{5/2}} \left( \frac{R_1 R_4}{R_1 + R_4} \right)^{1/2} + \frac{1}{(\hat{S}+2T/g)^{5/2}} \left( \frac{R_1 R_3}{R_1 + R_3} \right)^{1/2} \right] \quad (5)$$

where  $\hat{S} = 1 - \hat{w}_a - \hat{w}_b$ . The nonlinear governing equations (4) could be solved with and without dynamic terms.

**2.1. Static Analysis** Ignoring the acceleration and damping terms in equations (4) the static governing equations are:

$$\mathcal{L}_a(\hat{w}_{as}, V) = \frac{d^4 \hat{w}_{as}}{d\hat{x}^4} - (\alpha_1)_a \hat{F}_e - (\alpha_2)_a \hat{F}_V = 0$$

$$\mathcal{L}_a(\hat{w}_{bs}, V) = \frac{d^4 \hat{w}_{bs}}{d\hat{x}^4} - (\alpha_1)_b \hat{F}_e - (\alpha_2)_b \hat{F}_V = 0 \quad (6)$$

where subscript 's' is an indication of the static deflections of the nanotubes and  $\mathcal{L}_i$ 's are differential operators. Because of the nonlinearity of these equations, the solutions could be complicated and time consuming [16]. Therefore in order to solve them, it is tried to linearize them. Due to considerable value of  $\hat{w}$  with respect to initial gap, especially for high applied voltages,

linearizing the equations about undeflected straight positions may cause considerable errors. Therefore, to minimize the value of these errors, the method of step by step increasing the applied voltage is proposed [6]. It is assumed that  $\widehat{w}^k$  is the deflections of the microbeam due to the applied voltages  $V^k$ . So, by increasing the applied voltages to a new value

$$V^{k+1} = V^k + \delta V \quad (7)$$

The resultant deflections could be written as:

$$\begin{aligned} \widehat{w}_{as}^{k+1} &= \widehat{w}_{as}^k + \delta \widehat{w}_{as} = \widehat{w}_{as}^k + \psi_a(\widehat{x}) \\ \widehat{w}_{bs}^{k+1} &= \widehat{w}_{bs}^k + \delta \widehat{w}_{bs} = \widehat{w}_{bs}^k + \psi_b(\widehat{x}) \end{aligned} \quad (8)$$

Substituting Equation (8) into Equation (6) gives the governing equations in step  $(k+1)^{\text{th}}$

$$\begin{aligned} \mathcal{L}_a(\widehat{w}_{as}^{k+1}, V^{k+1}) &= \frac{d^4 \widehat{w}_{as}^{k+1}}{d\widehat{x}^4} - (\alpha_1)_a \widehat{F}_e^{k+1} - (\alpha_2)_a \widehat{F}_V^{k+1} = 0 \\ \mathcal{L}_b(\widehat{w}_{bs}^{k+1}, V^{k+1}) &= \frac{d^4 \widehat{w}_{bs}^{k+1}}{d\widehat{x}^4} - (\alpha_1)_b \widehat{F}_e^{k+1} - (\alpha_2)_b \widehat{F}_V^{k+1} = 0 \end{aligned} \quad (9)$$

Now by considering a small value of  $\delta V$ , it is expected that  $\psi(\widehat{x})$  would be small enough, hence using of Calculus of Variation theory and Taylor's series expansion about  $\widehat{w}^k$ , and applying the truncation to first order of it for suitable value of  $\delta V$ , it is possible to obtain desired accuracy. So the linearized equations to calculate  $\psi(\widehat{x})$  can be expressed as:

$$\begin{aligned} \mathcal{L}_a(\psi_a, \psi_b) &= \frac{d^4 \psi_a}{d\widehat{x}^4} - (\alpha_1)_a \left[ \frac{\partial \widehat{F}_e}{\partial \widehat{w}_{as}^k} \psi_a + \frac{\partial \widehat{F}_e}{\partial \widehat{w}_{bs}^k} \psi_b + \frac{\partial \widehat{F}_e}{\partial V} \delta V \right] \\ &- (\alpha_2)_a \left[ \frac{\partial \widehat{F}_V}{\partial \widehat{w}_{as}^k} \psi_a + \frac{\partial \widehat{F}_V}{\partial \widehat{w}_{bs}^k} \psi_b \right] = 0 \\ \mathcal{L}_b(\psi_b, \psi_a) &= \frac{d^4 \psi_b}{d\widehat{x}^4} - (\alpha_1)_b \left[ \frac{\partial \widehat{F}_e}{\partial \widehat{w}_{as}^k} \psi_a + \frac{\partial \widehat{F}_e}{\partial \widehat{w}_{bs}^k} \psi_b + \frac{\partial \widehat{F}_e}{\partial V} \delta V \right] \\ &- (\alpha_2)_b \left[ \frac{\partial \widehat{F}_V}{\partial \widehat{w}_{as}^k} \psi_a + \frac{\partial \widehat{F}_V}{\partial \widehat{w}_{bs}^k} \psi_b \right] = 0 \end{aligned} \quad (10)$$

In order to solve equation (10), the Galerkin based reduced order model is used where  $\psi_a$  and  $\psi_b$  are expressed as:

$$\psi_a(\widehat{x}) = \sum_{j=1}^{\infty} m_j \varphi_j(\widehat{x}) \quad (11)$$

$$\psi_b(\widehat{x}) = \sum_{j=1}^{\infty} n_j \varphi_j(\widehat{x})$$

where  $\varphi_j$  is the  $j^{\text{th}}$  free vibration mode shape of a cantilever nanobeam. Substituting Equation (11) into Equation (10) and multiplying both sides by  $\varphi_i$ , they could be written as:

$$\begin{aligned} \int_0^1 \varphi_i(\widehat{x}) \mathcal{L}_a \left( \sum_{j=1}^N m_j \varphi_j(\widehat{x}), \sum_{j=1}^N n_j \varphi_j(\widehat{x}) \right) d\widehat{x} &= 0 \\ \int_0^1 \varphi_i(\widehat{x}) \mathcal{L}_b \left( \sum_{j=1}^N m_j \varphi_j(\widehat{x}), \sum_{j=1}^N n_j \varphi_j(\widehat{x}) \right) d\widehat{x} &= 0 \end{aligned} \quad (12)$$

Taking into account the orthogonality of the mode shapes, the nanotubes equations take a set of algebraic equations with unknown  $m_j$  and  $n_j$ 's.

Solving these equations will take  $\psi_a$  and  $\psi_b$  in each step  $k$ . Then, by substitution of the results into Equation (8),  $\widehat{w}_{as}$  and  $\widehat{w}_{bs}$  are obtained for the applied voltage  $V$ .

**2.2. Dynamic Analysis** When the exciting voltage is imposed suddenly (as a step DC voltage) the inertia effects of the nanotubes comes into view and they are deflected beyond their static equilibrium positions. Thus, the dynamic pull-in voltage is smaller than the static pull-in value as the nanotubes reach the critical pull-in gap sooner than in the static analysis. Taking into account the dynamic and damping terms, the equations of the nanotubes could have the following forms:

$$\begin{aligned} \frac{\partial^4 \widehat{w}_{ad}}{\partial \widehat{x}^4} + \frac{\partial^2 \widehat{w}_{ad}}{\partial t^2} + \widehat{c}_a \frac{\partial \widehat{w}_{ad}}{\partial t} &= \\ (\alpha_1)_a \widehat{F}_e + (\alpha_2)_a \widehat{F}_V &= F_a(V, \widehat{w}_{ad}, \widehat{w}_{bd}, g) \\ \frac{\partial^4 \widehat{w}_{bd}}{\partial \widehat{x}^4} + \frac{\partial^2 \widehat{w}_{bd}}{\partial t^2} + \widehat{c}_b \frac{\partial \widehat{w}_{bd}}{\partial t} &= \\ (\alpha_1)_b \widehat{F}_e + (\alpha_2)_b \widehat{F}_V &= F_b(V, \widehat{w}_{ad}, \widehat{w}_{bd}, g) \end{aligned} \quad (13)$$

where  $F_a$  and  $F_b$  are the nonlinear electrostatic

and van der Waals forces acting on the arms, and subscript  $d$  indicates the dynamic deflections. In order to solve the dynamic equations the Galerkin reduced order method is employed. Considering finite number ' $N$ ' of modes, the approximate dynamic deflections can be written as:

$$\widehat{w}_{ad}(\widehat{x}, \widehat{t}) \cong \sum_{j=1}^N \varphi_j(\widehat{x}) q_j(\widehat{t}) \quad (14)$$

$$\widehat{w}_{bd}(\widehat{x}, \widehat{t}) \cong \sum_{j=1}^N \varphi_j(\widehat{x}) p_j(\widehat{t})$$

where  $q_j(\widehat{t})$  and  $p_j(\widehat{t})$  are the generalized coordinates of the nanotube arms which have to be determined. Substituting Equation (14) into Equation (13) and multiplying both sides by  $\varphi_i(\widehat{x})$  as weight functions and integrating from  $\widehat{x}=0$  to 1, the following nonlinear ordinary differential equations are extracted:

$$\sum_{j=1}^n M_{ij} \ddot{q}_j(\widehat{t}) + \sum_{j=1}^n K_{ij} q_j(\widehat{t}) + \widehat{c}_a \sum_{j=1}^n c_{ij} \dot{q}_j(\widehat{t}) = (F_a)_i \quad (15)$$

$$\sum_{j=1}^n M_{ij} \ddot{p}_j(\widehat{t}) + \sum_{j=1}^n K_{ij} p_j(\widehat{t}) + \widehat{c}_b \sum_{j=1}^n c_{ij} \dot{p}_j(\widehat{t}) = (F_b)_i$$

where  $M$ ,  $K$ , and  $c$  are the mass, stiffness and damping matrices respectively, and  $F_a$

$$M_{ij} = \int_0^1 \varphi_i \varphi_j d\widehat{x}; \quad K_{ij} = \int_0^1 \varphi_i \varphi_j^{iv} d\widehat{x}; \quad c_{ij} = \int_0^1 \varphi_i \varphi_j d\widehat{x}$$

$$(F_a)_i = \int_0^1 \varphi_i F_a(V, \widehat{w}_{ad}, \widehat{w}_{bd}, g) d\widehat{x} \quad (16)$$

$$(F_b)_i = \int_0^1 \varphi_i F_b(V, \widehat{w}_{ad}, \widehat{w}_{bd}, g) d\widehat{x}$$

Due to the complexity of the self excited nonlinear Equations (15), they are solved step by step in time domain. In other words at each step of discrete time the nonlinear forcing vectors are calculated based on the results of previous step. In the analysis, if the time steps are chosen small enough acceptable results could be obtained.

### 3. NUMERICAL RESULTS

In this section some static and dynamic simulations are performed for various dimensions and specifications of the nanotubes in symmetric and asymmetric conditions. At first, to validate the proposed method some experimental data from previous papers are presented and compared. In an experiment where the arms length were  $2.5 \mu\text{m}$  and the initial gap between them was  $780 \text{ nm}$  and Young's modulus has been taken  $1 \text{ TPa}$ , Akita *et al* [12] plotted the load tip deflections curve of the arms. Due to practical limitations in measuring the diameter of the arms, they estimated it numerically as  $13.3 \text{ nm}$ . Based on energy method and using the same specifications *Ke et. al.* [14] found an effective diameter of  $11.6 \text{ nm}$ . Dequesnes *et. al* [17] employed the same data and using a lumped model, found the effective diameter to be  $10.9 \text{ nm}$ . To show the effectiveness of the proposed method, the same dimensions and specifications are used where the Galerkin-based SSLM method is employed to extract the results. The simulations results with the experimental data of reference [12] are plotted in Figure 2, where the effective diameter of the arms is found to be  $11.82 \text{ nm}$ . The static simulation result shows that the diameter identified by the proposed method is close to the extracted diameters and is consistent with possible metrology errors. The results of different methods are summarized in Table 1.

Also, in Reference [17], the result of a lumped model with the simulation results based on MD model has been compared.

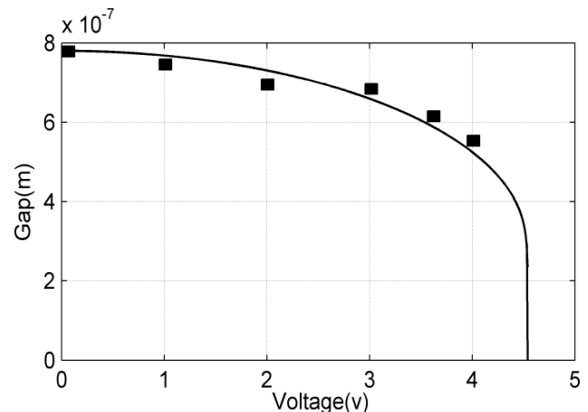


**Figure 2.** Tip deflection as a function of applied voltage based on experimental data (symbols ■) from [12] and present method.

**TABLE 1.** Comparison of different methods in perdition of the nanotube effective diameter.

Different methods	Akita- [12]	Deguesnes- [17]	C.-H. Ke- [14]	Proposed method
Effective diameter	13.3Nm	10.9Nm	11.6Nm	11.82Nm

In order to show the effectiveness of the present method, the MD model result is compared with the result of our numerical simulation method based on continuum model. The comparison for a nano-tweezer of radius 0.68 nm and length 20.7 nm with initial gap 3 nm is shown in Figure 3.

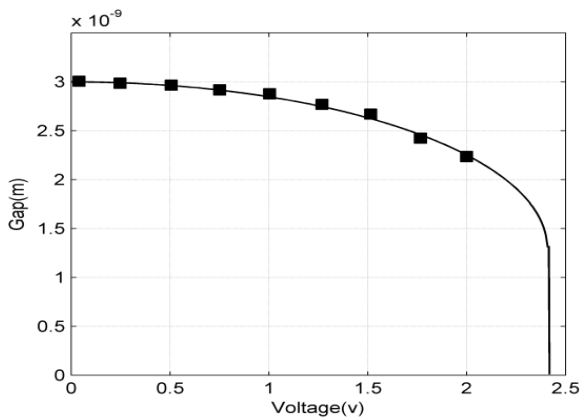


**Figure 3.** Tip deflection as a function of applied voltage based on MD model (symbols ■) [17] and present method.

After showing the effectiveness of the proposed method in solving the governing continuum model, some numerical simulations are presented to investigate the static and dynamic responses of nano-tweezers with and without symmetric nano-arms. In each case, the effects of some parameters of the CNT arms on the pull-in voltage are studied.

**3.1. Symmetric Arms** In the symmetric case where the CNT's of a nano-tweezer have the same geometry and specifications, the effects of their lengths, initial gap and diameters on the static and dynamic pull-in voltages are investigated. Figure 4 shows the effect of CNT length on the load tip deflection curves and related pull-in voltages. The other specifications of the CNT's are "gap( $g$ )=780nm,  $R_1=R_3=2$ nm,  $R_2=R_4=6$ nm and  $E_1=E_2=1$ TPa". It can be seen that by increasing the effective length of the arms the pull-in voltages decreases drastically. In dynamic case where the

exciting voltage is imposed suddenly as a step DC voltage, the pull-in conditions differ from the static case. The results of dynamic simulations for three different lengths with lower and higher than their pull-in voltages are shown in Figure 5. The results show that the instability voltage is lowered considerably with increasing the CNT length in both static and dynamic cases. This dependency is shown in Figure 6.

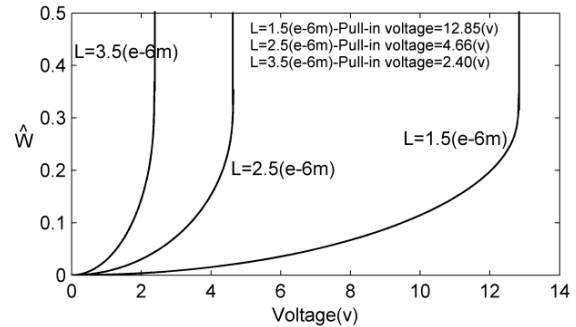


**Figure 4.** Effect of CNT length on the static load deflection curve and pull-in voltage

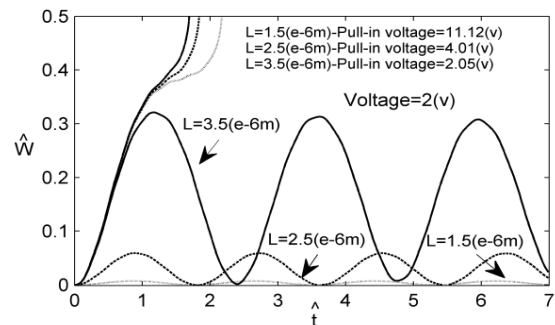


**Figure 5.** Effect of CNT length on the Dynamic response and dynamic pull-in voltage.

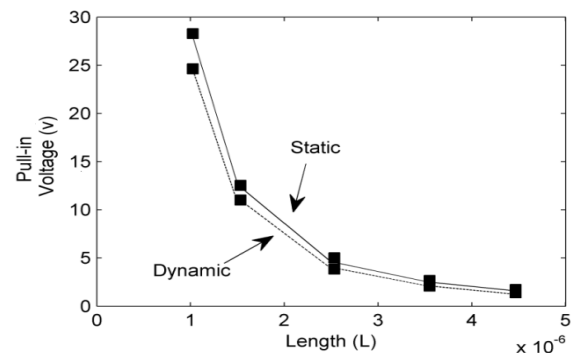


**Figure 6.** Effects of the CNT length on the static and dynamic pull-in voltages.

When the CNT's lengths are fixed as  $2.5\mu\text{m}$  and their initial gap is varied, the static load tip deflection curves are shown in Figure 7. The results show that the initial gap also affects the instability conditions considerably. In this case the diameters and Young's modulus are the same as the previous case. Taking into account the acceleration terms and imposing step DC voltages, the time history of the arm tip deflections are shown in Figure 8. It can be seen for a DC voltage lower than the pull-in one the initial gap changes the response amplitudes and frequencies considerably. The variations of the pull-in voltage for three different gaps are also shown in the figure. The critical conditions of the Figures 7 and 8 are summarized and plotted in Figure 9, where the dependencies of the static and dynamic pull-in voltages to the arms initial gaps are shown.

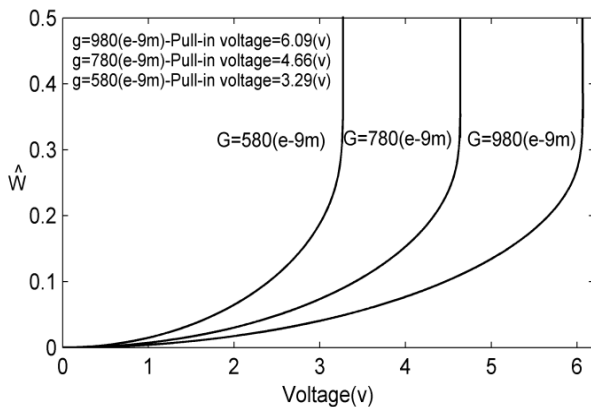


**Figure 7.** Effect of initial gap between the arms on the static load deflection curve and pull-in voltage.

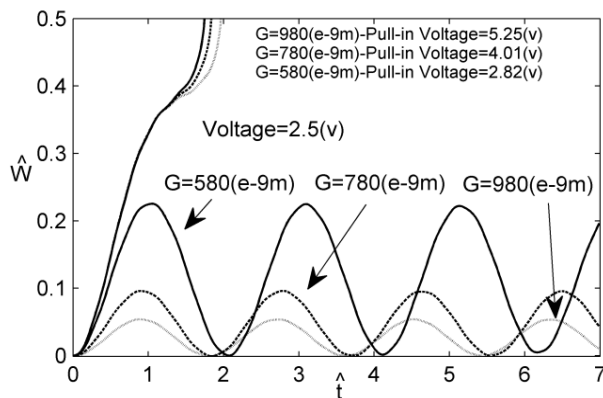


**Figure 8.** Effect of initial gap between the arms on the dynamic response and dynamic pull-in voltage.

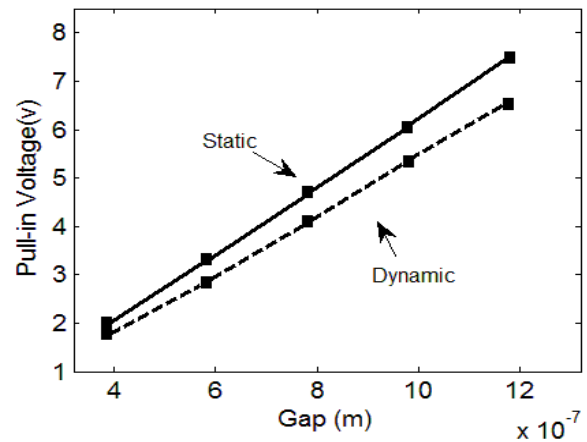


**Figure 9.** Effects of the initial gaps on the static and dynamic pull-in voltages.

Diameter of the nanotubes is the other important parameter which changes the instability conditions. Figure 10 shows the variations of the static and dynamic pull-in voltages as function of the outer nanotube diameters  $R_0$ . In this figure, the length of the tubes is  $2.5\mu\text{m}$  and their initial gap is  $780\text{nm}$ . As the diameter increases, the pull-in voltage also increases in the static and dynamic cases.

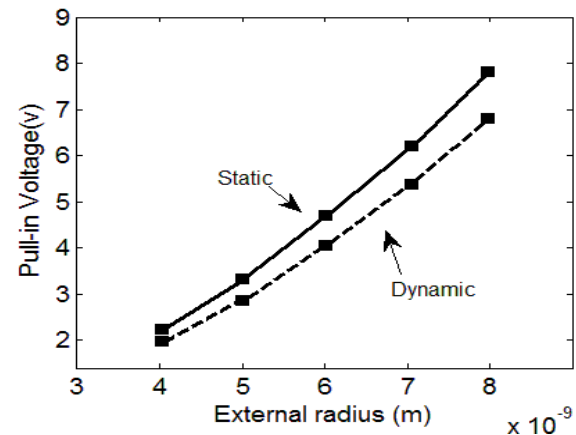


**Figure 10.** Effects of the nanotube radius on the static and dynamic pull-in voltages.

In the above simulations, due to large gaps (order of hundred nanometers), van der Waals forces do not play a significant role and the electrostatic force  $\hat{F}_e$  is dominated. However, if the initial gap is of the order of nanometers, the van der Waals forces could have considerable effects. By imposing a potential difference of 1 volt between the arms, variations of the ratio of force  $\hat{F}_V$  to the

total force  $\hat{F}_V + \hat{F}_e$  as function of the initial gap 'g' is plotted in Figure 11. It is inferred that the  $\hat{F}_V$  can be ignored in many applications, where the gaps are greater than 30 nm [13].

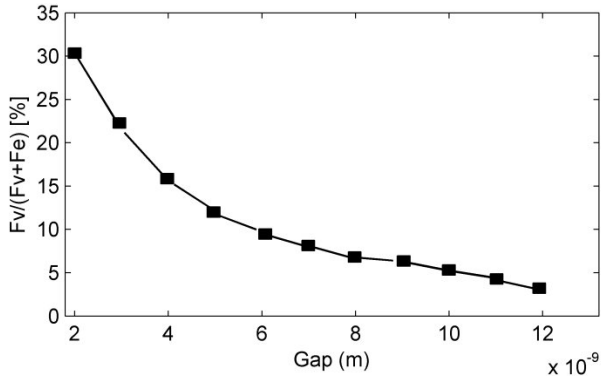


**Figure 11.** Contributions of the van der Waals force as function of initial gap

In the present simulations the damping effects which can become into view due to structural, thermal or squeeze effects is ignored. However, in real applications it may plays an important role in the stability and dynamic responses of a nano-tweezer. Figure 12 shows the effects of the damping near the pull-in conditions, where the imposed voltage is 4.01volts. It is seen that besides the stability conditions, it can affect the pull-in time significantly.

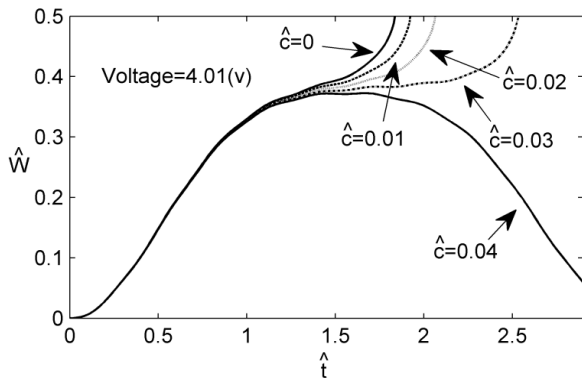


**Figure 12.** Effects of the damping on the dynamic response.

**3.2. Asymmetric Arms** In practical cases, the local weakness of the mechanical strength at the base of the arms of a nano-tweezer may be

different from each other. In addition, when the multiwalled carbon nanotubes are used as tweezing elements, the arms may have different layers and consequently different material properties. In these cases the two arms of a nano-tweezer could have different shapes at the closing stage [12]. In the following the effects of different radii and modulus of elasticity,  $E_i$ , of the arms on the static and dynamic responses are studied. Figure 13 shows the static tip deflection curves of the arms with same outer radius of 6 nm and different inner radii of 1 and 4 nm. In the simulation, the arms length is 2.5  $\mu\text{m}$  and initial gap is 780 nm. The dynamic response of the arms with imposing various level of applied voltages are shown in Figure 14. It can be seen that the asymmetry in closing of the arms can change the instability conditions, and consequently the manipulating process of the nano-tweezer significantly.

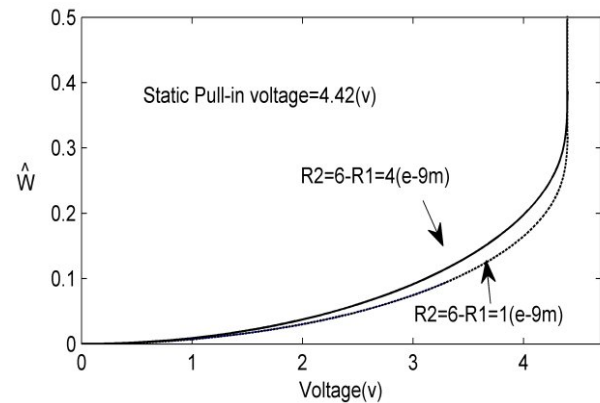


**Figure 13.** Asymmetric static tip load deflection curves of the arms due to different inner radii.

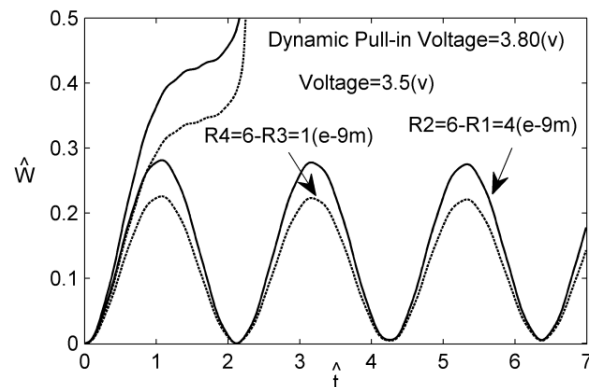


**Figure 14.** Asymmetric dynamic tip load deflection curves of the arms due to different inner radii.

As well, in attaching the arms to their supports or constructing the arms, their bending rigidities,  $E_i$ , may be varied. So, in applying voltage difference between the arms they could have different responses in static and dynamic conditions. For illustration, the results of simulations with different bending rigidities of the arms are shown in static and dynamics conditions in Figures 15 and 16 respectively. The different dynamic responses and different pull-in voltages are shown these figures.

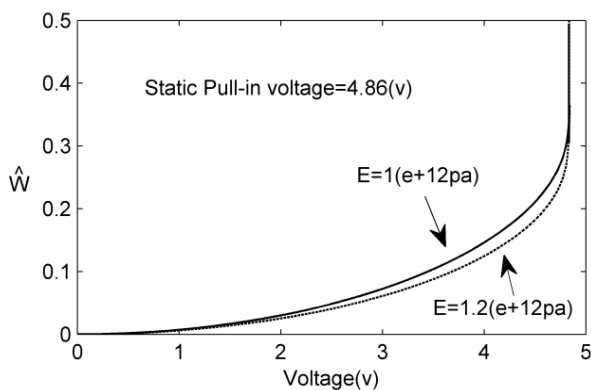


**Figure 15.** Asymmetric static tip load deflection curves of the arms due to different rigidities.

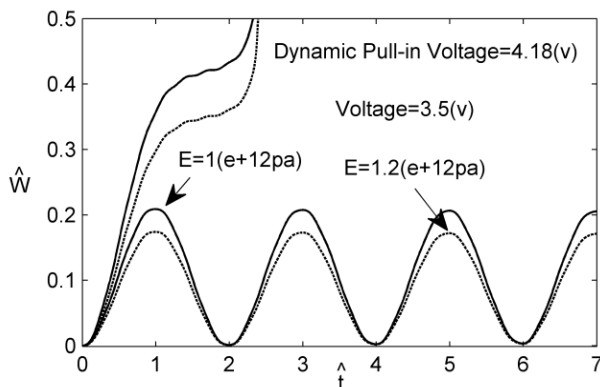


**Figure 16.** Asymmetric dynamic tip load deflection curves of the arms due to different rigidities.

#### 4. CONCLUSION

Using a continuum model and imposing electrostatic actuation, static and dynamic responses of nano-tweezers were studied. The nonlinear governing equations were solved employing SSLM and Galerkin projection

methods. Comparing the results of the static analysis with the existing experimental data shows the effectiveness of the proposed method. The effects of some parameters such as the length and diameters of the arms and the initial gap on the statics and dynamics of closing response were also studied. The effects of the damping ratio on the pull-in voltages and pull-in times of the nano-tweezer are reported. Finally, the effects of differences in the arms, mechanical strength at their bases or differences in the bending rigidities were simulated. The results showed that in addition to the instability, the manipulation process can be affected by asymmetric arms. The results could be useful for accurate design of nano-tweezers.

#### 5. REFERENCES

1. Iijima, S., "Helical microtubules of graphic carbon", *Nature*, Vol. 354, (1991), pp. 56–58.
2. Sazonova, V. and Yaish, Y., Ustunel, H., Roundy, D., Arias, T. and McEuen, P., "A tunable carbon nanotube electromechanical oscillator", *Nature*, Vol. 431, (2004), pp. 284-287.
3. Kinaret, J., Nord, T. and Viefers, S., "A carbon-nanotube-based nanorelay", *Applied Physics Letters*, Vol. 82, No. 8, (2003), pp. 1287-1289.
4. Lee, S. W., Lee, D. S., Morjan, R. E., Jhang, S., Sveningsson, M., Nerushev, O., Park, Y. and Campbell, E., "A Three-Terminal Carbon Nanorelay", *Nano Letters*, Vol. 4, (2004), pp. 2027-2030.
5. Baughman, R. H., Cui, C. X., Zakhidov, A. A., Iqbal, Z. and Barisci, J. N., "Carbon Nanotube Actuators", *Science*, Vol. 284, (1999), pp. 1340–1344.
6. Zarei, O. and Rezaadeh, G., "A Novel Approach to Study of Mechanical Behavior of NEM Actuators Using Galerkin Method", *International Journal of Nanosystems*, Vol. 1, No. 2, (2008), pp. 161-169
7. Fennimore, A. M., Yuzvlnsky, T. D., Han, W. Q., Fuhrer, M. S., Cummings, J. and Zettl, A., "Rotational actuator based on carbon nanotubes", *Nature*, Vol. 424, (2003), pp. 408-410.
8. Rueckes, T., Kim, K., Joselevich, E., Tseng, G. Y., Cheung, C. L. and Lieber, C. M., "Carbon Nanotube-Based Nonvolatile Random Access Memory for Molecular Computing", *Science*, Vol. 289, (2000), pp. 94–97.
9. Anand, Y. J., Harsha, S. P. and Sharma, S. C., "Vibration signature analysis of single walled carbon nanotube based nanomechanical sensors", *Physica E*, Vol. 42, (2010), pp. 2115–2123.
10. James, G. and Boyd, J. L., "Deflection and pull-in instability of nanoscale beams in liquid electrolytes", *Journal of Colloid and Interface Science*, Vol. 356, (2011), pp. 387–394.
11. Kim, P. and Lieber, C. M., "Nanotube and

- Nanotweezers", *Science*, Vol. 286, (1999), pp. 2148 - 2150.
12. Akita, S., Nakayama, Y., Mizooka, S., Takano, Y., Okawa, T., Miyatake, Y., Yamanaka, S., Tsuji, M. and Nosaka, T., "Nanotweezers consisting of carbon nanotubes operating in an atomic force microscope", *Applied Physics Letters*, Vol. 79, No. 11, (2001), pp. 1691-1693.
  13. Lee, J. and Kim, S., "Manufacture of a nanotweezer using a length controlled CNT arm", *Sensors and Actuators A*, Vol. 120, (2005), pp. 193-198.
  14. Ke, C. H., Pugno, N., Peng, B. and Espinosa, H. D., "Experiments and modeling of carbon nanotube-based NEMS devices", *Journal of mechanics and physics of solids*, Vol. 53, (2005), pp. 1314-1333.
  15. Pugno, N., Ke, C. H. and Espinosa, H. D., "analysis of doubly clamped nanotube devices in finite deformation regime", *Journal of Applied Mechanics*, Vol. 72, (2005), pp. 445-449.
  16. Wang, G. W., Zhang, Y., Zhao, Y. P. and Yang, G. T., "Pull-in instability study of carbon nanotube tweezers under the influence of van der Waals forces", *Journal of Micromechanics and Microengineering*, Vol. 14, (2004), pp. 1119-1125.
  17. Dequesnes, M., Rotkin, S. V. and Aluru, N. R., "Calculation of pull-in voltages for carbon-nanotube-based nanoelectromechanical switches", *Nanotechnology*, Vol. 13, (2002), pp. 120-131.
  18. Dequesnes, M., Tang, Z. and Aluru, N. R., "Static and dynamic analysis of carbon nanotube-based switches", *Journal of engineering materials and technology*, Vol. 26, (2004), pp. 230-237.
  19. Ramezani, A., "Stability analysis of electrostatic nanotweezers ", *Physica E*, Vol. 43 (2011), pp. 1783–1791.